

# 3. Numerical Simulation Reactor Research Project

Fusion plasmas are complex systems which involve a variety of physical processes interacting with each other across wide ranges of spatiotemporal scales. In the National Institute for Fusion Science (NIFS), we are utilizing the full capability of the supercomputer system, Plasma Simulator, and propelling domestic and international collaborations in order to conduct the Numerical Simulation Reactor Research Project (NSRP). Missions of the NSRP are i) to systematize understandings of physical mechanisms in fusion plasmas for making fusion science a well-established discipline and ii) to construct the Numerical Helical Test Reactor, which is an integrated system of simulation codes to predict behaviors of fusion plasmas over the whole machine range.

The Plasma Simulator is to be replaced in July 2020 to a new model (Fig. 1). It consists of 540 computers, each of which is equipped with 8 “Vector Engine” processors. The 540 computers are connected with each other by a high-speed interconnect network. The computational performance of the new Plasma Simulator is 10.5 petaflops. The capacities of the main memory and the external storage system are 202 terabytes and 32.1 petabytes, respectively. The nickname of the new Plasma Simulator is “Raijin (雷神)” which means a god of thunder.

Presented below in Figs. 2 and 3 are examples of successful results from collaborative simulation researches in 2019–2020 on ballooning and kink modes in the PLATO tokamak and on nonlinear saturation mechanism of toroidal ETG turbulence. Also, highlighted in the following pages are achievements of the NSRP on energetic-particle physics, neoclassical and turbulent transport, peripheral plasma transport, multi-hierarchy physics, and simulation science basis.

(H. Sugama)



Fig. 1 The new Plasma Simulator, “Raijin (雷神)”

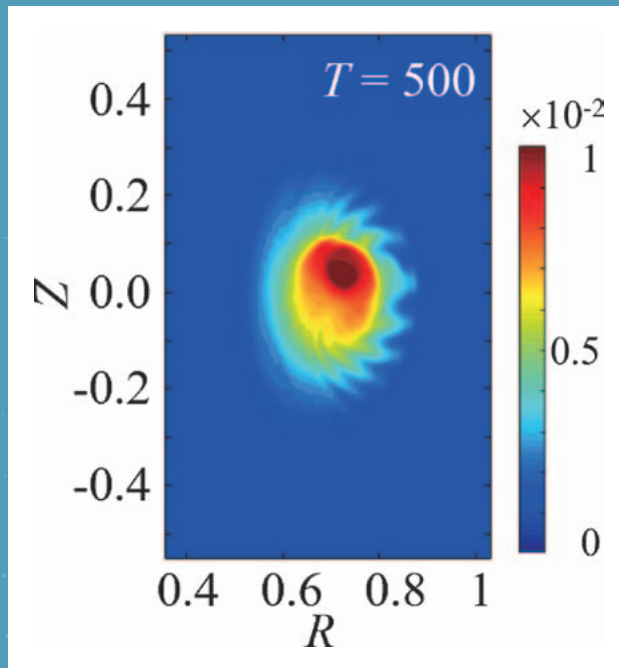


Fig. 2 Emergence of kink instability with existence of ballooning instability on the poloidal cross section of the PLATO tokamak obtained by nonlinear MHD simulation using the MIPS code [presented by N. Kasuya (Kyushu University)]. Reference: S. Tomimatsu, *et al.*, Plasma Fusion Res. (2020) in press.

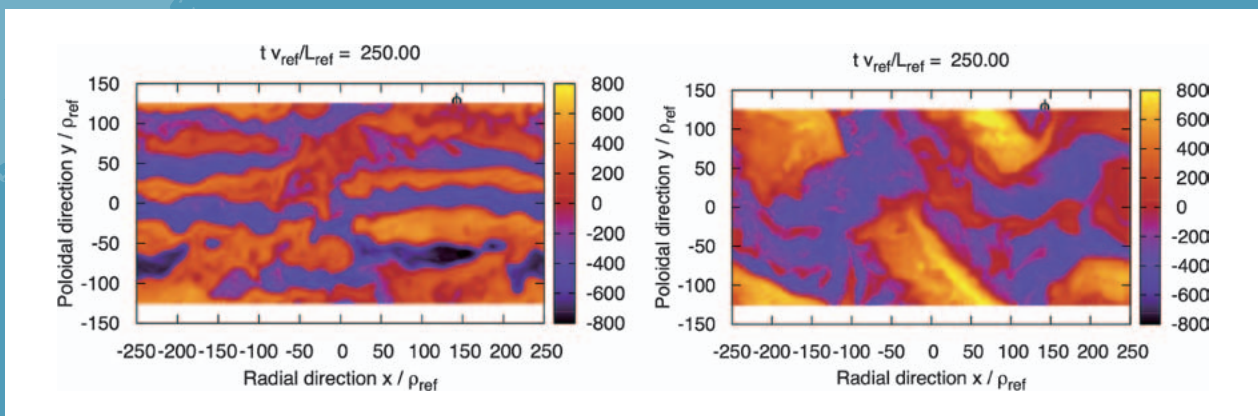


Fig. 3 Snapshots of the electrostatic potential in the nonlinear saturation phase of the toroidal ETG turbulence obtained by gyrokinetic simulation using the GKV code for the cases with “adiabatic” (left) and kinetic (right) ions [presented by T.-H. Watanabe (Nagoya University)]. In the latter case, finite radial wavenumber modes strongly modulate the ETG streamers.

# Energetic Particle Physics

## Highlight

### Extended kinetic magnetohydrodynamic hybrid simulations with thermal and fast ions clarify the fast-ion transport due to multiple Alfvén eigenmodes

The closure problem of magnetohydrodynamics (MHD) remains unresolved for collisionless high-temperature plasmas. A new hybrid simulation model where the gyrokinetic particle-in-cell simulation method is applied to both thermal and fast ions has been developed [1]. The new simulation model was implemented and applied to fast-ion driven instabilities in tokamak plasmas. Energy channeling from fast ions to thermal ions through the interaction with Alfvén eigenmodes (AEs) was demonstrated by the simulations. The real frequency and the spatial profile of the AEs are in good agreement with those given by the standard hybrid simulation for energetic particles interacting with an MHD fluid.

The distribution functions of fast ions and thermal ions are analyzed in detail during the nonlinear evolution of the multiple AEs. Figure 1 compares the fast-ion distribution function perturbations among the linear growth phase of the primary AE, the saturation phase of the primary AE, the nonlinear phase with the growth of the secondary AE, and the final phase for co-going and counter-going particles to the plasma current. The resonant orbits are also shown in Fig. 1 with the resonance poloidal numbers labeled in the figure. We see in Fig. 1 (c) and (g) that the poloidal mode number of the distribution function perturbations are different from those for the linear growth phase shown in Fig. 1 (a) and (e). This indicates that the secondary mode is excited leading to the further transport of fast ions and the global flattening of the distribution functions shown in Fig. 1 (d) and (h).

[1] Y. Todo *et al.*, “Extended magnetohydrodynamic hybrid simulations with kinetic thermal and fast ions for instabilities in toroidal plasmas”, in the 46th European Physical Society Conference on Plasma Physics (July 8–12, 2019, Milan, Italy).

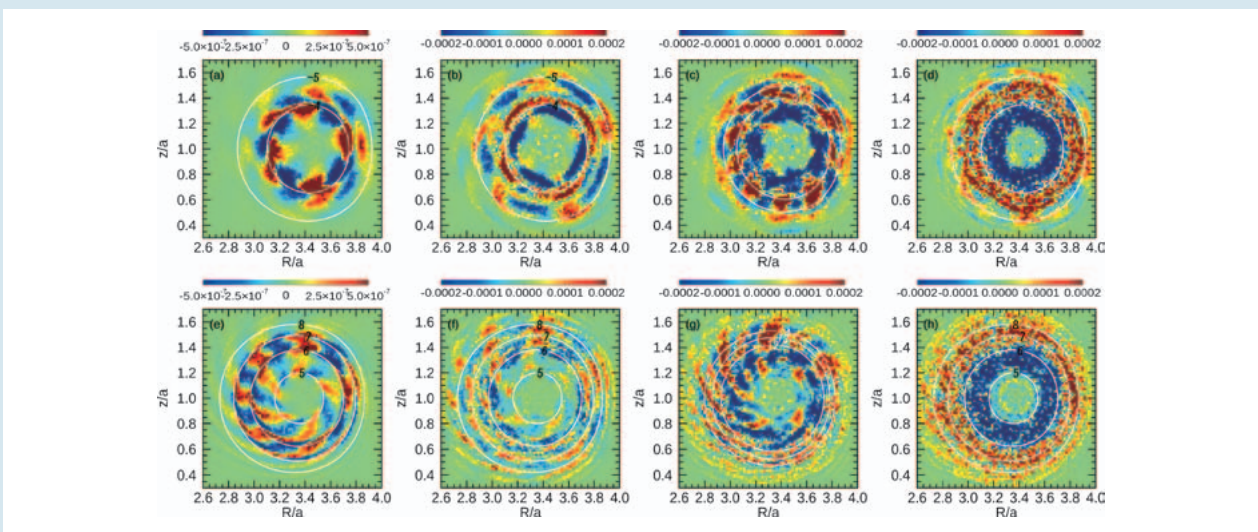


Fig. 1 Fast-ion distribution function perturbations in the evolution of multiple Alfvén eigenmodes (AEs) for (a, e) linear growth phase of the primary AE, (b, f) saturation phase of the primary AE, (c, g) nonlinear phase with the growth of the secondary AE, and (d, h) final phase for (a-d) co-going particles and (e-h) counter-going particles to the plasma current. In the final phase shown in (d) and (h), the distribution functions are globally flattened due to the transport by the multiple AEs.

(Y. Todo)

## Simulation of Alfvén eigenmodes destabilized by energetic electrons in tokamak plasmas

Alfvén eigenmodes (AEs) driven by energetic electrons were investigated via hybrid simulations of an MHD fluid interacting with energetic electrons [2]. The investigation focused on AEs with the toroidal number  $n=4$ . Both energetic electrons with centrally peaked beta profile and off-axis peaked profile are considered. For the centrally peaked energetic electron beta profile case, a toroidal Alfvén eigenmode (TAE) propagating in the electron diamagnetic drift direction was found. Figure 2 shows the resonance condition between energetic electrons and the TAE. The TAE is mainly driven by deeply trapped energetic electrons. It is also found that a few passing energetic electrons spatially localized around rational surfaces can resonate with the mode. For the off-axis peaked energetic electron beta profile case, an AE propagating in the ion diamagnetic drift direction was found when a  $q$ -profile with weak magnetic shear is adopted. The destabilized mode has a frequency close to the second Alfvén gap and two main poloidal harmonics  $m=6$  and  $m=8$ , which indicate that this mode is an ellipticity-induced Alfvén eigenmode. Passing energetic electrons and barely trapped energetic electrons are responsible for the mode destabilization.

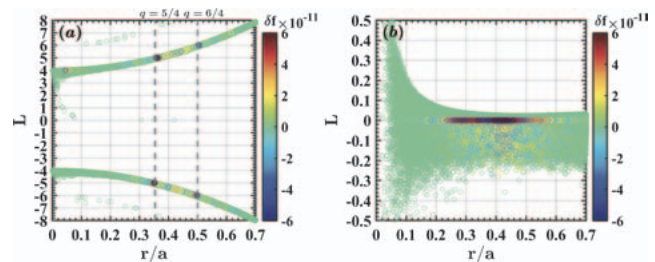


Fig. 2 (a) Resonance condition for (a) passing energetic electrons and (b) trapped energetic electrons along radial coordinate. Each marker in the figure represents one computational particle and all particles are included. Particle positions in the mid-plane during one bounce/transit period are stored and the average value of the stored positions is used as the particle location in the figure [2].

[2] Jialei Wang *et al.*, “Simulation of Alfvén eigenmodes destabilized by energetic electrons in tokamak plasmas”, to appear in *Nucl. Fusion* **60** (2020).

(Jialei Wang)

## Systematic investigation of energetic-particle-driven geodesic acoustic mode channeling

Energetic-particle-driven geodesic acoustic modes (EGAMs) channeling in the Large Helical Device (LHD) plasmas are systematically investigated for the first time using MEGA which is a hybrid simulation code for energetic particles interacting with a magnetohydrodynamic (MHD) fluid [3]. EGAM channeling behaviors are analyzed under different conditions. During the EGAM activities without frequency chirping, EGAM channeling occurs in the linear growth stage but terminates in the decay stage after the saturation. During the EGAM activities with frequency chirping, EGAM channeling occurs continuously. Also, lower frequency EGAM makes the energy transfer efficiency ( $E_{\text{ion}}/E_{\text{EP}}$ ) higher, because the interactions between lower frequency mode and bulk ions are stronger. This is confirmed by changing the energetic particle pressure and energetic particle beam velocity, as shown in Fig. 3. Moreover, higher bulk ion temperature makes the energy transfer efficiency higher. In addition, under a certain condition, the energy transfer efficiency in the deuterium plasma is lower than that in the hydrogen plasma. Based on the simulations described above, suggestions are given for experiments. The higher neutral beam injection (NBI) power, the lower NBI velocity, the higher number of perpendicular injected particles, the higher bulk ion temperature, and the wider bulk ion temperature profile are probably applicable strategies for improving the observation of EGAM channeling.

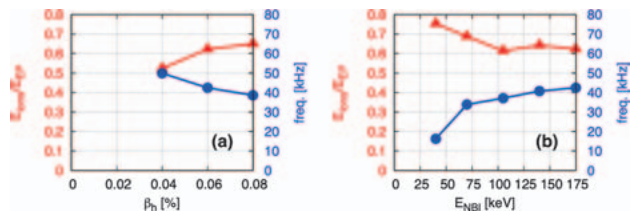


Fig. 3 The energy transfer efficiency (triangles) and EGAM frequency (circles) versus (a) the energetic particle pressure and (b) the beam energy.

[3] H. Wang *et al.*, “The systematic investigation of energetic-particle-driven geodesic acoustic mode channeling using MEGA code”, to appear in *Nucl. Fusion* **60** (2020).

(Hao Wang)



# Transport simulation for helical plasmas by use of gyrokinetic transport model

## Highlight

**The transport simulation results explain the experimental results for the temperature profiles, where the ion temperature gradient mode is unstable.**

The transport simulation is performed in helical plasmas by use of two kinds of the reduced models [1] for the kinetic electron response (heat diffusivity and quasilinear flux models) for the turbulent transport. The neoclassical transport is included in the transport simulation. For the turbulent transport, the instability due to the ion temperature gradient (ITG) is studied. The additional modeling of the quantity related with the mixing length estimate and the zonal flow decay time in the diffusivity models is done. Electron heat diffusivity model is adopted to the transport simulation for the additional modeling by the normalized characteristic length for the ion temperature gradient. Furthermore, electron quasilinear flux model is installed to the transport simulation codes by the ratio of the electron quasilinear heat flux to the ion quasilinear heat flux, where the ion heat flux is evaluated by the heat diffusivity model. The ion heat diffusivity model is also installed into the integrated transport code for simulating evolutions of the plasma profiles in the LHD, when the additional modeling by the characteristic length for the ion temperature gradient is used.

The electron temperature profiles of the transport simulation results by the electron heat diffusivity model and the quasilinear flux model are compared with the experimental observation result in the LHD in figure 1 (a). The ion temperature profile of the dynamical transport simulation by use of the ion heat diffusivity model for the kinetic electron response is also compared with the LHD experimental result in figure 1 (b) [2].

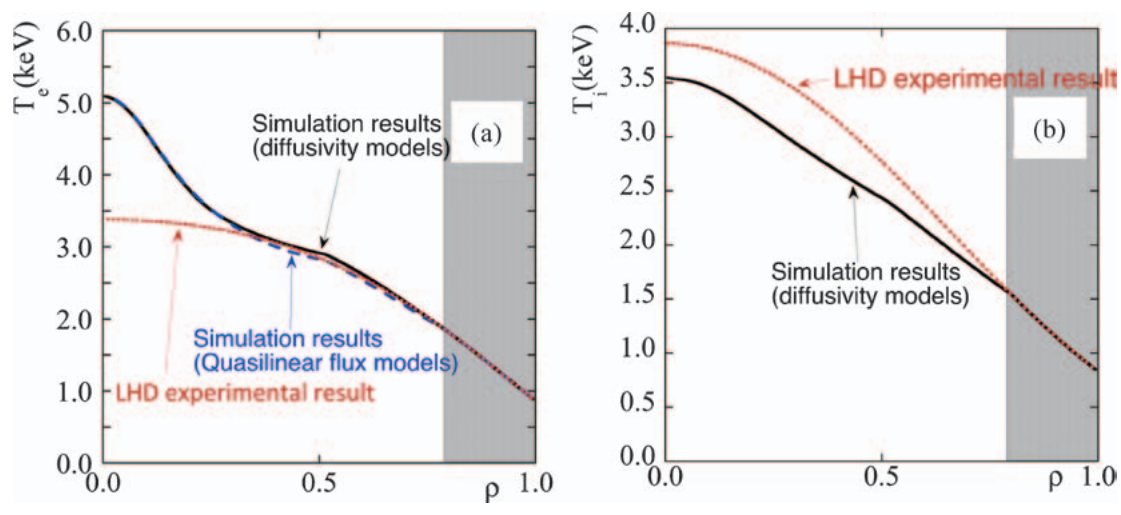


Fig. 1 The radial profiles of  $T_e$  are shown. The solid and dashed lines represent the electron temperature profiles for the simulation results, using the heat diffusivity model and the quasilinear flux model, respectively. The dotted line indicates the experimental results. (b) The  $T_i$  profiles are shown. The solid line represents the ion temperature for the simulation results. The dotted line indicates the experimental results at  $t=2.2$ s in the LHD.

[1] S. Toda *et al.*, Phys. Plasmas **26**, 012510 (2019).

[2] S. Toda *et al.*, Plasma Fusion Res. **14**, 3403061 (2019).

## Gyrokinetic simulations for turbulent particle transport of multi-ion-species plasma with impurity hole structure in LHD system

The turbulent particle transport of multi-ion-species plasma with the impurity hole structure in the LHD system and their plasma profile sensitivities are investigated by the flux-tube gyrokinetic simulations [3]. In the plasma, the turbulent heat transport flux of each species has slightly different dependences on the radial gradients of the plasma temperatures and densities. On the other hand, while the particle transport is determined satisfying the ambi-polar condition between electrons and all ion species, the particle fluxes have quite different dependences for different species as shown in Fig. 2. In the LHD plasma having the hole density structure of the impurity carbon ions, it is found that the turbulent particle flux of the carbon ions is radially inward-directed robustly for the wide ranges of the radial gradient profiles of the temperatures and densities. Furthermore, we also found that there are clear balance relations in the turbulent particle fluxes between the pair of hydrogen and helium ions, and the pair of the electrons and carbon ions.

(M. Nunami)

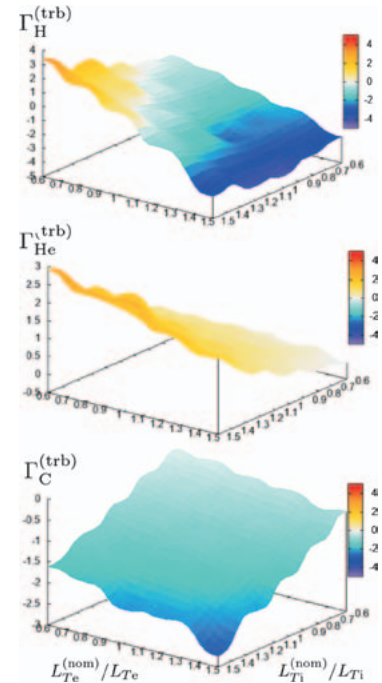


Fig. 2 Temperature gradient length dependences of turbulent particle fluxes for hydrogen  $\Gamma_H^{(trb)}$ , helium  $\Gamma_{He}^{(trb)}$ , and carbon  $\Gamma_C^{(trb)}$  ions.

## Development of global neoclassical transport simulation for multi-ion-species plasma

To study the impurity transport process and hydrogen isotope effect, neoclassical transport simulation code needs to be capable of handling the collisional diffusion process in multi-ion-species plasma. We developed a new linearized Landau collision operator, which is applicable to multi-ion-species plasma, and implemented to a global neoclassical  $\delta f$ -PIC code FORTEC-3D [4]. The new collision operator satisfies the conservation properties, self-adjointness, and H-theorem. As a verification, very good agreement in the damping process of the mean flow and temperature fluctuation was demonstrated between FORTEC-3D and gyrokinetic code GKV as shown in Fig. 3. FORTEC-3D was applied to study the effect of potential variation on flux surface on impurity transport to study the impurity-hole phenomenon. It is revealed that the global simulation is essential for the evaluation of the impurity transport [5].

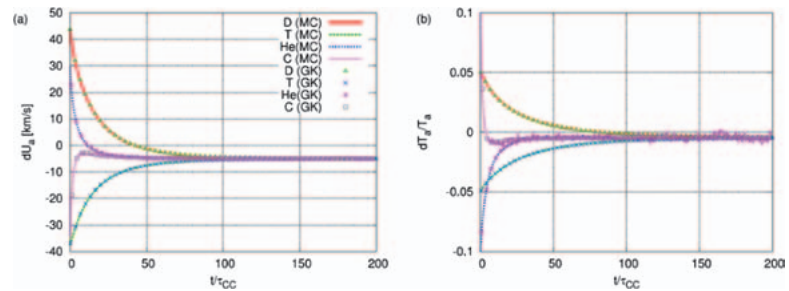


Fig. 3 Comparisons on the collisional damping process of the mean flow and temperature in 4 ion species plasma calculated by FORTEC-3D (curves) and GKV (points) [4].

[3] M. Nunami, M. Nakata, S. Toda, and H. Sugama, *Phys. Plasmas* **27**, 052501 (2020).

[4] S. Satake, M. Nakata, T. Pianpanit *et al.*, *Comp. Phys. Comm.* **255**, 107249 (2020).

[5] K. Fujita, S. Satake, R. Kanno *et al.*, *J. Plasma Phys.*, *in press*.

(S. Satake)

## Peripheral transport physics

### Highlight

# Nonlinear MHD simulation confirmed pellet injection drives edge MHD instability

The effect of pellets on the global magnetohydrodynamic (MHD) dynamics of the Large Helical Device (LHD) has been analyzed with the MIPS code [1], which is a nonlinear MHD simulation code [2]. A pellet ablation model based on the neutral gas shielding model has been implemented to the MIPS code. Excitation of MHD modes by the three-dimensionally localized pressure perturbation caused by the pellet injection has been observed. MHD instabilities depends on the pellet size.

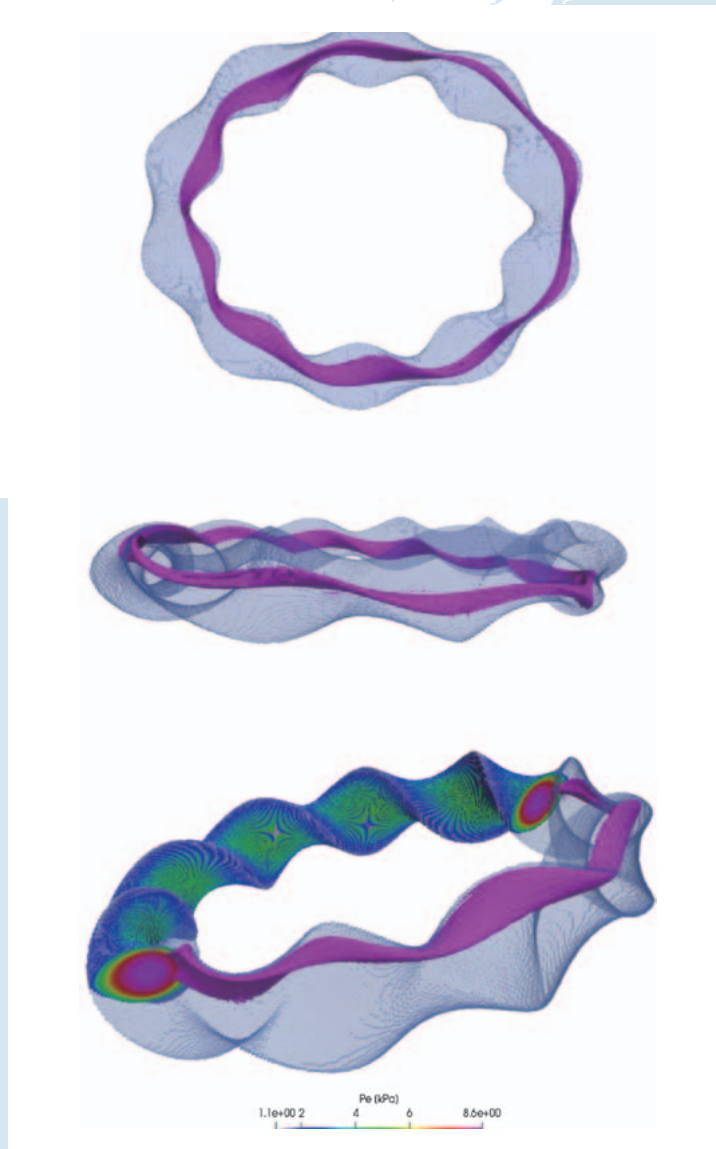


Fig. 1 The pellet cloud profile at the maximum ablation for the pellet size of  $2.0 \times 10^{21}$  particles/pellet.

Pellet injection is an experimentally proven method of plasma refueling in tokamak and stellarator plasmas. Pellet injection into the plasma is also used for plasma control, i.e. ELM (Edge Localized Mode) mitigation for tokamaks by means of the excitation of magnetohydrodynamic (MHD) activities. In stellarators, also ELM-like instabilities are frequently observed, and those instabilities must be controlled and mitigated. Besides the benefit of pellet injection in terms of the edge plasma instability control, plasma instabilities which are inimical phenomena via pellet injection are problems that have come into focus simultaneously. For considering those problems, the global MHD dynamics has been analyzed with the MIPS code, which solves the full MHD equations coupled with a pellet ablation model. The pellet ablation model, which is based on the neutral gas shielding (NGS) model, has been implemented in MIPS. There are two important features in our implementation of the model into the MIPS code. The first feature is that the pellet is modeled as a localized adiabatic time-varying density source. The pellet density source is toroidally and poloidally localized. The second feature is that the pellet moves at fixed speed and direction. An excitation of MHD modes by the three-dimensionally localized pressure perturbation originating from the pellet injection has been observed. Figure 2 shows the time evolution of the magnetic energies for the cases with no pellet and pellet sizes. If no pellets, the mode was not excited. The modes of  $m/n = 2/1$ ,  $m/n = 2/2$ ,  $m/n = 2/3$  are plotted with solid lines, dashed lines and dotted lines, respectively. The amplitude of the excited MHD energies is proportional to the size of the injected pellet, larger pellets result in larger amplitudes of the excited MHD activity.

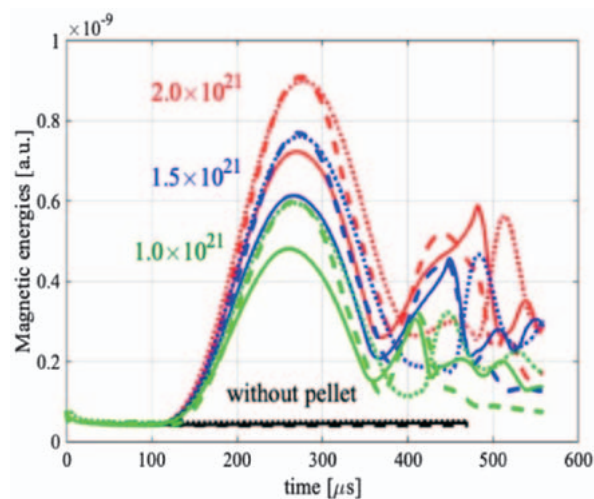


Fig. 2 Time evolution of the magnetic energies for the case of absence of the pellet,  $1.0 \times 10^{21}$  (green lines),  $2.0 \times 10^{21}$  (blue lines),  $2.0 \times 10^{21}$  (red lines). The pellet injection velocity is  $1000 \text{ m s}^{-1}$  for all cases. The modes of  $m/n = 2/1$ ,  $m/n = 2/2$ ,  $m/n = 2/3$  are plotted in the solid lines, dashed lines and dotted lines, respectively.



## Towards whole-volume kinetic modeling of helical fusion devices including the edge region

### Highlight

## Development of a global gyrokinetic particle-in-cell code utilizing unstructured meshes

It is crucial to evaluate plasma transport in the edge region near the divertor as well as in the core region with closed magnetic field lines. The edge plasma transport affects the durability of fusion devices through divertor heat load and also the plasma confinement through impurity contamination. While these two regions are not physically separated, conventional simulation studies focused on either of them because field line structures and plasma conditions are significantly different. We are developing a global gyrokinetic code toward whole-volume modeling of Helical fusion devices [1]. This code will enable us to perform kinetic simulations on edge plasma transport dynamically coupled with the plasma confinement in the core region. The simulation code originates from “X-point Gyrokinetic Code (XGC)” developed for Tokamaks with axisymmetric geometries in Princeton Plasma Physics Laboratory. XGC utilizes particle-in-cell scheme with unstructured meshes potentially applicable outside the nested flux surfaces. We have extended XGC to non-axisymmetric geometries by implementing new mesh generation schemes, three-dimensional spline interpolation, and the VMEC equilibrium data interface. As the first step, we have successfully demonstrated fundamental plasma phenomena, such as neoclassical transport accompanied by a radial electric field and linear growth of ion temperature gradient mode in the core region of Large Helical Device (LHD). The novel simulation schemes and related benchmark tests were presented in the IAEA Fusion Energy Conference (FEC 2018) [2].

We are continuing to develop the code to include the edge region of LHD within the present simulation framework. A smooth magnetic field equilibrium with the edge region is obtained from the VMEC equilibrium through a virtual casing method in EXTENDER code. The unstructured mesh is constructed by numerical field line tracing in this equilibrium. We have tested elemental procedures in the time step cycles, such as particle orbit tracing and finite element field solver [2]. We will improve the field calculation and the mesh generation schemes to calculate the self-consistent time evolution of perturbed electrostatic fields in the edge region in the next step.

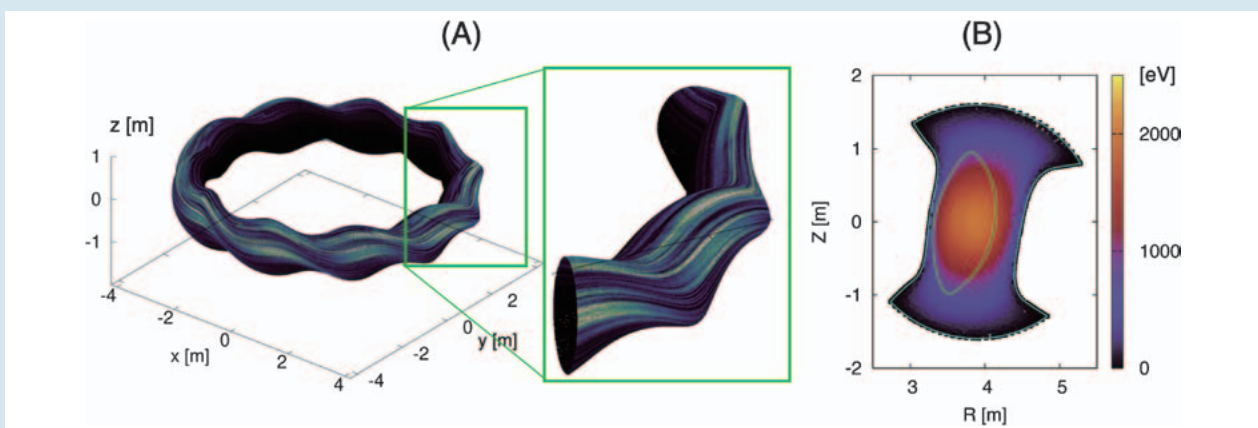


Fig. 1 Electrostatic potentials in Large Helical Device obtained from the developed code, XGC-S. (A) Electrostatic potential in linear ITG simulation for the core region. (B) Electrostatic potential generated from a uniform charge density in the entire region.

[1] T. Moritaka, R. Hager, M. Cole, S. Lazerson, C-S. Chang, S. Ku, S. Matsuoka, S. Satake and S. Ishiguro, *Plasma* **2**, 179–200 (2019).

[2] T. Moritaka, R. Hager, M. Cole, S. Laserzon, S. Satake, C-S. Chang, S. Ku, S. Matsuoka, S. Ishiguro, Proceedings of the 27th IAEA Fusion Energy Conference, 2018.

## Three-dimensional effect of particle motion on plasma filament dynamics

We have shown with the three-dimensional electrostatic particle-in-cell simulation that the particle motion influences plasma filament dynamics three-dimensionally. The intermittent filamentary plasma structure, which has been observed in the boundary layers of various magnetic confinement devices, is radially transported by the dipolar electrostatic potential structure formed in the filament cross-section. When the ion-to-electron temperature ratio  $T_i/T_e$  is higher, the ion gyro motion upsets the balance in the dipolar potential structure. Such an unbalanced potential structure induces the poloidal symmetry breaking in the filament propagation [3]. Furthermore, in the high  $T_i$  case, the pre-sheath potential drop on the hill side in the dipolar potential structure becomes larger than that on the well side. The large pre-sheath drop on the hill side induces the strong dependence of the perpendicular electric field in the filament on the toroidal position. As shown in Fig. 2, the filament dynamics in the high  $T_i$  case, in which the poloidal symmetry breaking occurs as mentioned above, are significantly influenced by such a three-dimensional structure of the electric field [4].

[3] H. Hasegawa and S. Ishiguro, *Plasma* **1**, 61 (2018).

[4] H. Hasegawa and S. Ishiguro, *Phys. Plasmas* **26**, 062104 (2019).

(H. Hasegawa)

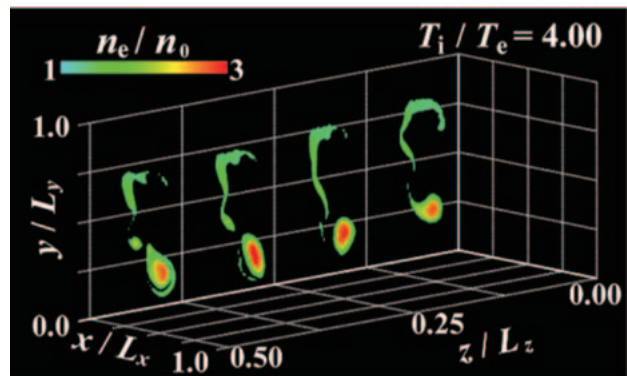


Fig. 2 Electron density distributions in the filament on four poloidal cross-sections at  $z/L_z = 0.125, 0.25, 0.375,$  and  $0.5$  for the high ion temperature ( $T_i/T_e = 4$ ) case.

## Dependence of the ion heating on poloidal and toroidal fields in magnetic reconnection

By means of two-dimensional electromagnetic particle simulations, we have investigated ion heating mechanism in magnetic reconnection. In 2017, we reported that ring-shaped ion velocity distributions are formed in the downstream of reconnection and that ions are effectively heated [5].

We have further explored this effective heating process and then have found incomplete ring-shaped, i.e., circular-arc-shaped velocity distributions in some cases. It is noted that a ring is an arc with the central angle of  $2\pi$ . According to our theory for the effective heating associated with the circular-arc-shaped structure of velocity distribution, the ion effective temperature depends on the radius and the central angle of an arc. Our particle simulations demonstrate two types of dependence of the ion heating [6]. Figure 3 (a) shows that (i) the ion heating energy is proportional to the square of the poloidal magnetic field. On the other hand, it is represented in Fig. 3 (b) that (ii) as the toroidal magnetic field is higher, the effective temperature is lower, but this dependence becomes small for very high toroidal field. The dependence (i) and (ii) are in good agreement with tendencies reported in STs such as TS-6, Univ. Tokyo.

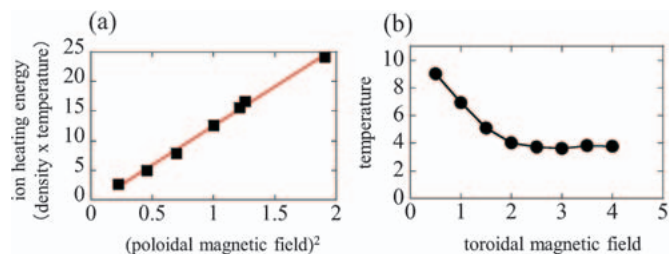


Fig. 3 Dependence of the ion effective heating on (a) the poloidal magnetic field and (b) the toroidal magnetic field. These tendencies are consistent with ones reported in ST experiments.

[5] S. Usami, R. Horiuchi, and H. Ohtani, *Phys. Plasmas* **24**, 092101 (2017).

[6] S. Usami, R. Horiuchi, H. Ohtani, Y. Ono, M. Inomoto, H. Tanabe, *Phys. Plasmas* **26**, 102103 (2019).

(S. Usami)

# Visualization of the Plasma Shape in a Force Free Helical Reactor, FFHR

### Highlight

## A plasma shape is visualized by using the magnetic field lines calculated in the equilibrium plasma for optimization of a three-dimensional shape design of the component in the reactor.

FFHR generates twisted magnetic fields confining the plasma at the center of the vessel. To achieve a high usage of the energy generated from the nuclear fusion, the blankets are set closely to the plasma. At meanwhile, a gap between two blankets is arranged for the magnetic field lines to go through to the divertor for the online removal of impurities from the plasma. It should be noticed that these components need to be accurately designed as the energy for nuclear fusion will be lost when the plasma tends to attack the blankets.

Previously, a shape of the component in the reactor was designed considering a structure of the magnetic field line in two-dimensional cross section at the discrete toroidal angle, that is, the Poincare plots of the magnetic field lines. However, the magnetic field line has a three-dimensional (3D) structure and the plasma particle has a spread region of the Larmor radius around the magnetic field. Therefore, it is necessary to work three-dimensionally with the plasma for optimization of a 3D shape design of the component in the reactor. It will enable us to check interference between the plasma and the 3D design data of the components in the reactor. Marching cubes algorithm is a sequential-traversal method commonly used in medical imaging technology for generating isosurface described by a scalar field [1]. Here, we have combined Marching cubes method with our approach and built a 3D model of the plasma shape.

Firstly, through applying MGTRC [2], the information of each magnetic field line is recorded. Secondly, we bring in the Larmor radius. Each magnetic field line is consisted of line segments. Further, a line segment is defined by two points. With these two points and their normal vectors calculated by the magnetic field, we can get two circular profiles representing the Larmor radius. By connecting averagely divided points on the two circles with straight lines. A tube-like structure is obtained. Figure 1 shows a magnetic field line with the other lines serving as Larmor radius. Subsequently, the position of all those lines can be transformed to the volume data.

To provide the volume data, the number of the magnetic field lines which go across each cube is recorded. A 3D digital differential analyzer [3] is applied for making sure that cubes between two relatively far points can be counted into the sum. After that, vertex values of a cube can be decided by averaging the recorded numbers belonging to its adjacent cubes. Recently, we reconsider the above method, proposing to calculate the distance between a vertex of a cube and the magnetic field line which goes across it. It is proved that the new method can provide a better visualization result. Figure 2 shows the model of the plasma shape.

Finally, we match the plasma model with the FFHR model for checking the interference.

This research has been organized into a paper and is about to be published in 'Journal of Advanced Simulation in Science and Engineering' [4]. In the future, we would like to improve our method according to the request from the domain expert in NIFS.

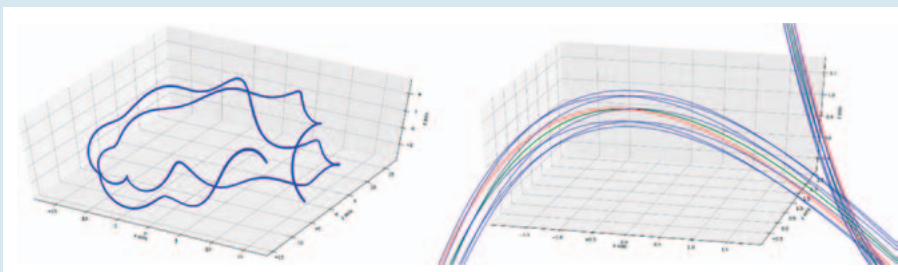


Fig. 1 On the left is a piece of magnetic field line. On the right is a part of the line after zooming in. In which, the green line refers to the original traced magnetic field line, the red and blue ones respectively are the starting line and those lines obtained by rotating the starting line, representing the Larmor radius.



Fig. 2 The 3D model of the plasma shape generated from specialized Marching cubes method.

[1] T. S. Newman, H. Yi, *Computers & Graphics*, **30**, 854 (2006).

[2] Project webpage. <https://github.com/yasuhiro-suzuki/MGTRC>.

[3] A.Y. Chang, Polytechnic University, Department of Computer and Information Science, (2001).

[4] H. Kunqi *et al.*, *J. Adv. Sim. Sci. Eng.*, **7**, 151 (2020).

(K. Hu and K. Koyamada, Kyoto Univ., H. Ohtani)

## Development of in-situ visualization library “VISMO”

We have been developing an in-situ visualization library VISMO [1], which is provided as a module of Fortran2003 and is easily combined with simulation codes. The simulation size becomes larger scale, and the simulation researchers can get fruitful results from the big data because of the rapidly advanced computer technology. However, it becomes difficult to deal with such large data by the traditional interactive visualization method on the PC due to the data size. In order to solve the problem, in-situ visualization method is investigated. In the in-situ visualization method, the visualization code is inserted into the simulation code, the visualization process is performed on the supercomputer the simulation code runs, and the visualized results are outputted as form of image instead of raw data.

We have added several visualization functions to the VISMO library: 1) Visualization of particle with sphere whose color and radius are changeable according to the physical value, such as velocity. 2) Coloring of isosurface whose color indicates the other scalar value. 3) Arrow presenting vector field. Arrows are scattered in whole calculation region or they are put only in the region the researcher focuses on. 4) Designation of background color. 5) Correspondence to single-precision real number. We have also optimized the library for Plasma Simulator with optimization of transfer function and have developed an interface module for implementation of the library to the simulation code to increase the convenience for users.

In order to visualize the objects from various viewpoints, VISMO has a function in which the visualized objects are outputted as forms of point clouds [2,3]. The special viewer of the point cloud data was installed to CompleXscope (Fig. 1). The viewer was also ported to the head-mount display system by using CLCL library [4].

This library was implemented to the simulation codes in other research fields, such as quantum turbulence system [4] and Hall MHD system [5]. The figure in Ref. [5] was selected as Kaleidoscope in Physical Review E. These facts prove that the VISMO library can generate a high-quality figure.

- [1] N. Ohno and H. Ohtani, *Plasma Fusion Res.*, **9**, 3401071 (2014).
- [2] N. Ohno, H. Ohtani and W. Zhang, *ITC26* (2017).
- [3] N. Ohno and H. Ohtani, *The 8th AICS International Symposium* (2018).
- [4] S. Kawahara and A. Kageyama, *J. Adv. Sim. Sci. Eng.*, **6**, 234 (2019).
- [5] K. Yoshida, H. Miura, Y. Tsuji, *J. Low Temp. Phys.*, **196**, 211 (2019).
- [6] H. Miura, J. Yang, T. Gotoh, *Phys. Rev. E*, **100**, 063207 (2019).

(N. Ohno of Hyogo Univ., H. Ohtani, H. Miura and A. Kageyama of Kobe Univ.)



Fig. 1 VISMO viewer in CompleXscope.



## Current distribution optimization in electromagnet: Application to performance enhancement of superconducting linear acceleration system

As an alternative pellet injection system for a magnetic confinement fusion reactor, the Superconducting Linear Acceleration (SLA) system has been recently proposed. The SLA system is composed of an electromagnet and a pellet container to which a High-Temperature Superconducting (HTS) film is attached. The container is accelerated by the Lorentz force between the electromagnet and the HTS film. Therefore, in order to use the SLA system efficiently, it is indispensable to enhance the acceleration performance of a single electromagnet. To this end, by using the genetic algorithm [1], the current distribution in the electromagnet is optimized so as to maximize the acceleration performance. In the present study, the current distribution is represented by means of the on/off method [2], and the dynamic motion of the container is simulated by using the equivalent-circuit model [3].

According to the optimized result, the pellet velocity  $v$  is improved by a factor of 1.7 as compared with that for the homogeneous current distribution (see Fig. 1). Moreover, the cross section in which the electric current flows is reduced to 0.9. Therefore, the electric current should not be always applied to the entire electromagnet to achieve the enhancement of the acceleration performance.

- [1] K. Deb *et al.*, *IEEE Trans. Evol. Comput.*, **6** (2), pp. 182–197 (2002).
- [2] Y. Hidaka *et al.*, *IEEE Trans. Magn.*, **50** (2), 7015204 (2014).
- [3] T. Yamaguchi *et al.*, *J. Adv. Simul. Sci. Eng.*, **4** (2), pp. 209–222 (2019).

(T. Yamaguchi, SOKENDAI, T. Takayama, Yamagata Univ., H. Ohtani, N. Yanagi and A. Kamitani, Yamagata Univ.)

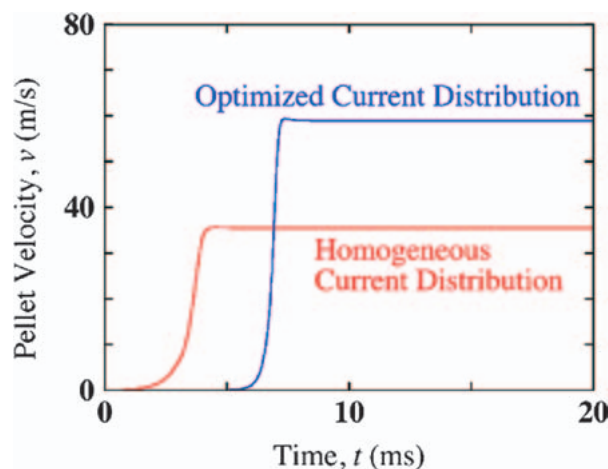


Fig. 1 Time dependences of the pellet velocity  $v$ . In this figure, the blue and red curves denote the values for the optimized current distribution and the homogeneous current distribution.

